Automated alignment in mask-free photolithography enabled by micro-LED arrays

M. Stonehouse, A. Blanchard, B. Guilhabert, Y. Zhang,✉
E. Gu, I. M. Watson, J. Herrnsdorf, and M. D. Dawson
Department of Physics, Institute of PhotonicsUniversity of Strathclyde, Glasgow, UK (E-mail: mark.stonehouse@strath.ac.uk)

✉**Correspondence**
Y. Zhang, Information Optoelectronics Research Institute, Harbin Institute of Technology at Weihai, Weihai, China.
Email: alexander.blanchard@strath.ac.uk

We present an automated control system for micro scale positioning, based on single pixel imaging and fluorescence. By projecting a chequerboard array of CMOS controllable μ-LEDs at a suitable wavelength, we are able to spatially locate, track and automatically align to fluorescent markers. Positioning is demonstrated with accuracy on the order of 20 μm. We present a maskless photo-lithography system using the automated control capability and a second μ-LED array to photocure customisable structures in photoresist with alignment referenced to the fluorescent markers.

Introduction: Automated control is a vital part of any large scale manufacturing capability. Microscale accurate and scalable automation are important in electronics and optoelectronics, where photolithography is often used for wafer patterning and device definition [1]. Mask-less photolithography is an increasingly important lithographic technique, thus far dominated by lasers and digital micromirror-based sources [2, 3]. Gallium nitride μ-LED (Micro-Light Emitting Diode) arrays of LED pixels with individual size from a few to a few 10′s of microns directly interfaced to CMOS (Complementary Metal–Oxide Semiconductor) control electronics, offers an attractive alternative [4, 5]. This is independent of pixel shape, with square [4, 5] and circular pixels used.

In this paper we demonstrate the potential of electronically-interfaced μ-LED arrays for alignment and control in mask-less photolithography. We specifically target microscale feature recognition and tracking capability to enable closed loop automated positioning. In our demonstration, spatio-temporally modulated illumination patterns at 450 nm aligned red-emitting fluorescent markers at arbitrary locations in the exposure plane, via CdSe/ZnS colloidal quantum dot (QD) microstructures or dye-doped microbeads. Photoresist patterns aligned to the markers were then made from a single 405 nm μ-LED in an array, and the programmed motion of an XYZ stage. We thus demonstrate a self-aligning, multi-step photolithographic capability, where μ-LED technology can locate and align to fluorescent positioning markers as well as define and expose further photo-patternable microscale features with these markers.

Optical Setup: A schematic of the optical setup used is shown in Figure 1; a variant of this set-up was used in our earlier work [6]. Note that while we used a CCD (Charge Coupled Device) camera here to give coarse spectral resolution, the imaging capability of the camera is not essential to our demonstration and is only used for monitoring and characterisation purposes. In the experiments below, we employ computational single-pixel imaging [7, 8] and thus the same results can be obtained with a single-element detector in place of the camera. Both μ-LED arrays used were fabricated in the Institute of Photonics and use gallium nitride. The μ-LED array used in the photo-curing process (LED2) is a 405 nm wavelength (corresponding to h-line), 16 × 16 pixel array of circular pixels 72 μm in diameter and 100 μm pitch, giving a 41% fill factor. The array used for structured illumination (LED1) is a 450 nm wavelength, 16 × 16 pixel 'chequerboard' array of square pixels of 99 μm edge length and 100 μm pitch, giving a 98% fill factor. FPGAs (Field Programmable Gate Arrays) 1 and 2 control the LED arrays. A series of lenses collimates and images the respective outputs of the arrays, demagnified by a 10× objective. The respective f-numbers of these lenses are f/10 for f1, f/2 for f2, and f/0.8 for both f3 and f4. The setup shown here results in projected μ-LED spot sizes of 20 μm, defining the positioning precision.

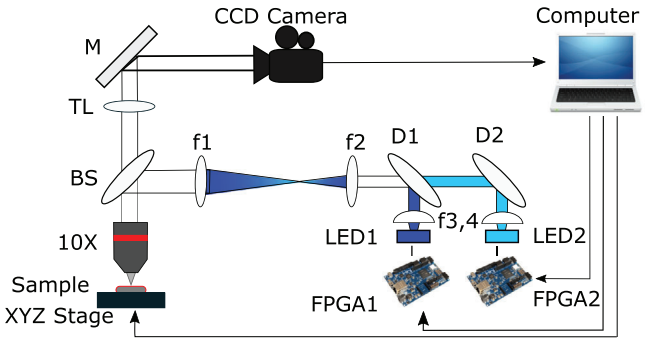

Fig. 1 *Schematic of the optical setup.*

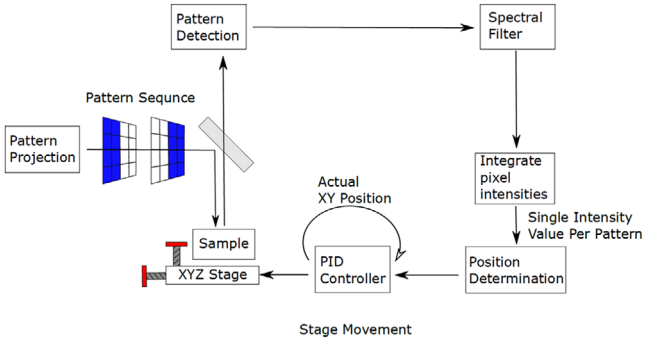

Fig. 2 *A schematic diagram showing how the pattern sequence is analysed*

Sample preparation: In this work we have used borosilicate glass slides as substrates for photopatterning, with two types of fluorescent markers: Red-emitting QD clusters, 20 μm in diameter, and fluorescent dyed microbeads, (Cospheric fluorescent red polyethylene microbeads), 10–22 μm in diameter. The term "marker" used refers to both the QD clusters and the microbeads, and the experiments shown here can be done with either marker. For microphotolithography, the QD clusters are added to the glass slide via an evaporation process to randomise the distribution of the clusters, to which resin was drop cast. The microbeads, in comparison, are directly added into a small amount of a UV (Ultra-Violet) sensitive acrylate resin (Anycubic clear UV resin), which is then drop cast onto the sample. This resin is light-sensitive enough at 405 nm for our purposes, whilst not curing when illuminated at 450 nm.

Automated positioning: The first step in our demonstration is automated positioning. The 450 nm wavelength μ-LED array projects a sequence of chequerboard-style binary illumination patterns onto the sample with the X,Y position of each individual LED representing a coordinate on the board and in the image plane. We can send a series of custom illumination patterns (known as a 'Moving Bars' sequence due to its form [, 9]) designed to create a unique temporally modulated 'fingerprint' at each location in the image plane. As these light patterns illuminate the sample they generate photoluminescence from any markers in the FOV (Field Of View) which can be detected remotely. Thus identifying the temporally modulated pattern of luminescence and relating this to the position-dependent modulation of the illumination permits the recognition and location of designated luminescent features within the FOV. The alignment process used the μ-LED array with a 98% fill factor, so that the FOV has a near-continuous light coverage.

Figure 2 shows the process sequence to obtain the marker coordinates, with Figure 3 showing camera images of representative frames from our pattern sequence. The blue light from our emitter is removed by a processing filter, leaving only the luminescence from the markers. This technique is not limited to blue light and/or red fluorescing markers, but rather can be applied to μ-LEDs emitting at any peak wavelength obtainable from gallium nitride devices in conjunction with markers capable of absorbing that light to produce longer-wavelength emission. Also shown in Figure 2 is the PID (Proportional Integral–Derivative) control loop whereby the software uses the current location of the marker to manipulate the sample-mounted XYZ mechanical stage during alignment, which is limited to 1 mm/s and 25.4 mm in the XY coordinate.

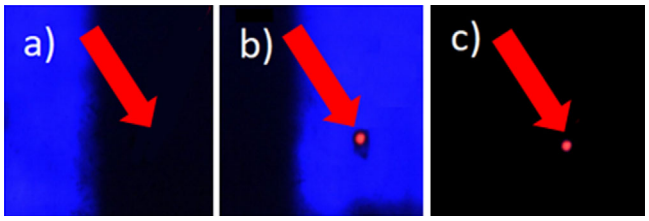

Fig. 3 *Images taken during the pattern detection. (a) An example illumination pattern where the alignment marker is not illuminated. (b) The inverse pattern of part (a) where the marker is illuminated. (c) The illumination pattern from part (b) after applying the spectral filter.*

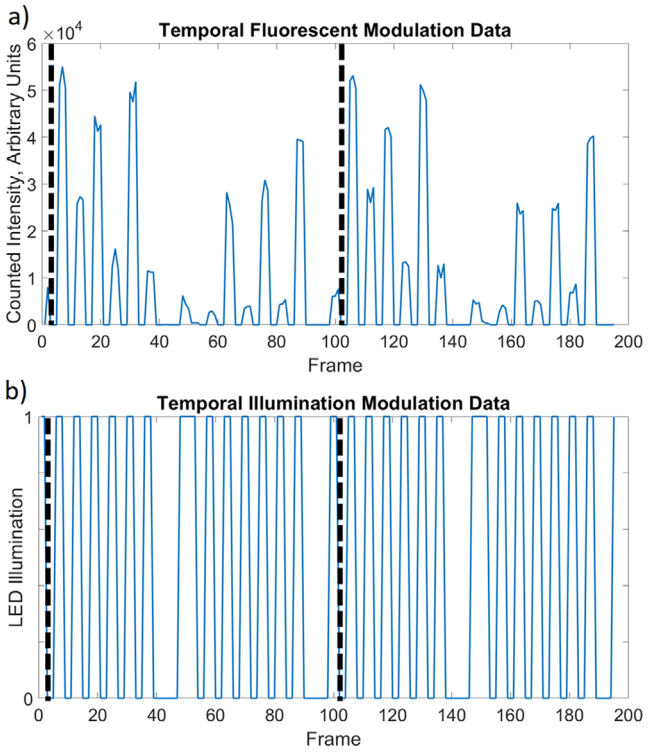

Fig. 4 *(a) Graph showing the temporal modulated fluorescent data for the system from the moving bars imaging sequence. The dotted lines indicate the start frame of the imaging sequence. (b) Graph showing the temporal illumination fluorescent data for the system from the moving bars imaging sequence. The dotted lines indicate the start frame of the imaging sequence.*

Temporally modulated fluorescent response: To check the fluorescent response of the markers, markers were placed randomly on the glass slide. An area with a single marker visible in the FOV of the 450 nm chequerboard array was then selected, and the full 'Moving Bars' sequence projected, with three camera frames recorded for each projected frame, recording the moving bars sequence twice. This captures the full pattern and records at least one usable frame for each projected frame.

The recorded frames are then spatially and spectrally filtered, only showing areas within the FOV of the LED1 array that record on the red channel of the CCD camera, showing the fluorescence. Then, the sum of the filtered image's intensity is calculated to simulate a single pixel detector such as a spectrometer. A rolling three frame sum is used to find the start frame; the smallest value for this sum indicates the start frame. If this start frame is calculated to be in the latter half of the recorded frames, it is shifted to use the full frame sequence.

Figure 4(a) shows the Temporal Fluorescent Modulated (TFM) data, the spectral response from each frame recorded for a marker. There is a pattern of three frames on and then three frames off, based on the position of the fluorescent marker and the 'fingerprint' pattern for that position, meaning that sequence will only be seen if the marker is in that position in the projected pattern. The different heights of the peaks reflect the relative overlap between the marker and projected LED pattern.

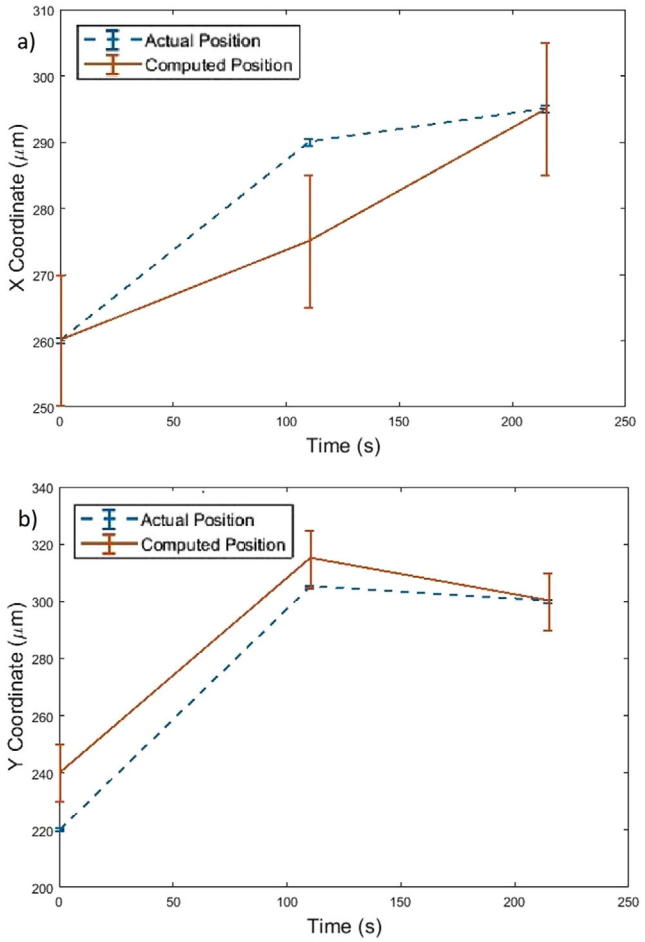

Fig. 5 *The movement of a fluorescent marker during the alignment process, for (a) the x-coordinate, and (b) the y-coordinate with respect to time. The computed position determined by the structured illumination process and the actual position as monitored by the camera through conventional imaging are shown. The error bars represent the coordinate grid resolution for the computed position and the pixel size and resolution of the CCD camera.*

The TFM data is used as the basis of the automated positioning system. The high difference between the on and off frames when the marker is fully in the FOV of the LED array in Figure 4(a) allows us to reduce the inherent errors when using this data for positioning purposes. A minimum search is applied onto the TFM data to find the position of the marker, which requires co-ordinates to be assigned in the FOV of the chequerboard array (LED1 in Figure 1). Figure 4(b) shows the temporal illumination modulation data, the illumination of the LED in each frame at the co-ordinate where the marker was calculated to be; a strong resemblance can be seen between this and the TFM data.

Marker trajectory: To test the automated positioning system, we again randomly dispersed markers, from which an area was manually selected in which only one marker was visible in the FOV of the 450 nm chequerboard array, then assigned a target co-ordinate to position to. The system was run until the marker was reported to be on the assigned coordinate, which was verified with the camera.

The mechanical stage controlled by the system's reference to the makers typically requires two sets of XY movements before successfully arriving at its target location, though this varies depending on the distance that the stage travels. This is due to inherent inaccuracies coming from the stage pico-motors, and that the fill factor of the LED output is not 100%. The highest number of cycles observed during alignment is from one corner to the opposite corner of the FOV (i.e. 630 μm distance) which required three detection and movement cycles. The absolute precision of the setup is dependent on the projected image size, rather than physical size of the μ-LEDs in the LED2 array.

Figure 5 shows a trajectory of the marker during alignment and its positional uncertainty, as verified by the camera. A marker was aligned

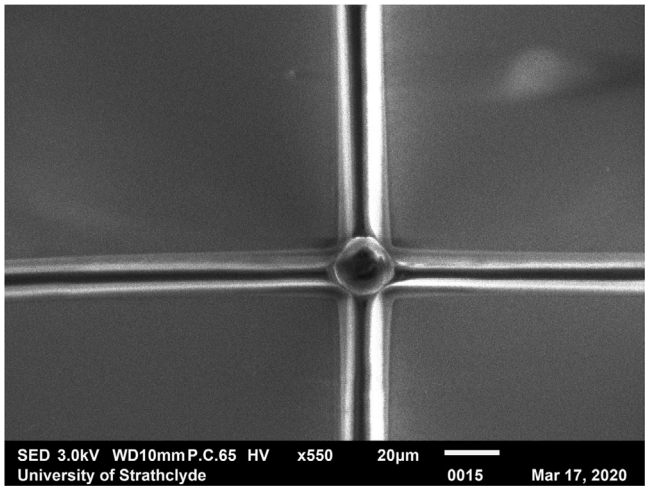

Fig. 6 *An SEM plane-viewed image of a cross with the alignment marker contained at the intersection. The marker at the centre is 21 μm in diameter.*

to coordinate (13,11) in the 16 × 16 array and we set its final location to (15,15). As shown, the positioning required only two sets of XY movements. This was repeated from corner to corner, requiring three sets of measurements instead. Note that this particular measurement was done with a 405 nm wavelength 16 × 16 array of circular pixels with a 41% fill factor, not the tessellated device with a 98% fill factor. This shows that the requirements on device uniformity and fill factor are not demanding, and any light which does not interfere with either the photo-resist or the fluorescent emission can be used. The higher fill factor of the chequerboard device results in lower inaccuracies during alignment compared to the circular device.

Aligned micro-photolithography: The second μ-LED array in our set-up, operating at 405 nm, is capable of mask-free exposure of resists and polymers patternable by h-line photolithography. To demonstrate the basic characteristics of this system under 10× demagnification as shown in Figure 1, we used a commercially available UV sensitive resin (Anycubic). This was then applied to the slide and spun to a film thickness of 9 μm. After alignment to the curing μ-LED array, the sample is cured with a dosage of approximately 181 mJ/cm^2. After photocuring, the sample was developed and cleaned.

The CMOS integrated μ-LED arrays allow spatial and temporal control of the emitted light through pulse width modulation, allowing control of the line width and feature size produced in the resist while keeping the writing speed constant. We achieved line thicknesses ranging from 14–35 μm, as measured by an optical profiler (Wyko NT1100), at a maximum height of 9 μm. By using smaller μ-LEDs, it is possible to achieve sub-micron resolution in such a system [10]. A reduced feature size can also be achieved by reducing the size of the projected μ-LEDs via stronger demagnification at the beam expander. However, by doing so, the FOV for the structured illumination will also be reduced, meaning that the tracking capability discussed earlier can only operate over a smaller area. Because of this, there is an inherent trade off between feature resolution and FOV. The write speed is limited by the stage speed to 1 mm/s and the stage range of 25.4 mm limits any patterns made.

We then combined this 405 nm direct writing with our active alignment capability demonstrated above. As a representative example, in Figure 6, we located and calibrated the system's positioning on a fluorescent marker using the patterned light sequences at 450 nm, and then wrote at 405 nm a cross pattern in resist which aligned with the marker at the crossing point. This shows the basic capability of this active alignment and direct writing system to produce aligned multi-step processing, for example, by encapsulating luminescent microstructures within or between separately microstructured polymer encapsulation or other functionality layers. Figure 6 uses environmental-mode operation of the SEM to suppress charging without application of any conductive coating, and was taken with a curing dose of 181 mJ/cm^2 from an LED duty cycle of 0.062, and a photoresist thickness of 9 μm.

Conclusion: We have developed and demonstrated an automated alignment system using a CMOS integrated 16 × 16 μ-LED array for structured illumination, measuring the fluorescent response of a microscale marker to a temporally dependent fingerprint signal. This positioning capability was then used as the basis for an automated alignment system, tracking the movement of the fluorescent marker to a pre-determined coordinate, taking two or three alignment cycles to do so. The positioning was then independently verified by a camera. The positioning system is used as the basis of a micro photo-lithography tool, using another CMOS integrated μ-LED array at a different wavelength for photo-curing at the aligned coordinate. The two arrays having different wavelengths means that the alignment does not affect the curing. Although we have used fluorescent markers here, it is also possible to align to reflective markers. Spectral analysis is possible at the detector end of the alignment process, demonstrated here with the RGB channels of the camera, but extendable to finer wavelength resolution taking advantage of the principles of single-pixel imaging. This can be explored with a spectrometer, aligning to narrow spectral signatures instead of a broad RGB signal for enhanced target identification from the spectral signatures.

Acknowledgments: The authors thank the Engineering and Physical Sciences Research Council for funding under grants EP/P0Z744X/2 and EP/S00175L/1. Data are available at https://doi.org/10.15129/ab01c91b-2c1e-4193-8221-fd071fb523e0. Thanks also go to Emma Butt for assistance with the SEM image, and Pedro Alves and Nicolas Laurand for the QDs.

Received: *8 March 2021* Accepted: *19 May 2021*
doi: 10.1049/ell2.12244

References

1 Levinson, H.J.: *Principles of lithography*, SPIE, Bellingham, WA (2019)
2 Dinh, D.H., Chien, H.L., Lee, Y.C.: Maskless lithography based on digital micromirror device (DMD) and double sided microlens and spatial filter array. *Optics Laser Technol.* **113**, 407–415 (2019)
3 Rydberg, C.: *Laser Mask Writers in Handbook of Photomask Manufacturing Technology*. Rizvi, S., (ed.). CRC Press, Boca Raton, USA (2005)
4 Herrnsdorf, J., et al.: Active-matrix GaN micro light-emitting diode display with unprecedented brightness. *IEEE Transactions on Electron Devices*. **62**(6), 1918–1925 (2015)
5 Elfström, D., et al.: Mask-less ultraviolet photolithography based on CMOS-driven micro-pixel light emitting diodes. *Opt Express*. **17**(26), 23522–23529 (2009)
6 Stonehouse, M., et al.: Microscale automated alignment and spatial tracking through structured illumination. In: IEEE Photonics Conference IPC, San Antonio, USA (2019)
7 Edgar, M.P., Gibson, G.M., Padgett, M.J.: Principles and prospects for single-pixel imaging. *Nat. Photonics* **13**(1), 13–20 (2019)
8 Xu, Z.H., et al.: 1000 fps computational ghost imaging using LED-based structured illumination. *Optics Express.* **26**(3), 2427–2434 (2018)
9 Herrnsdorf, J., Dawson, M.D., Strain, M.J.: Positioning and data broadcasting using illumination pattern sequences displayed by LED arrays. *IEEE Trans. Commun.* **66**(11), 5582–5592 (2018)
10 Guilhabert, B., et al.: Sub-micron lithography using InGaN micro-LEDs: mask-free fabrication of LED arrays. *IEEE Photonics Technol. Lett.* **24**(24), 2221–2224 (2012)